

Coherent control of atomic spin currents in a double well

H. T. Ng¹ and Shih-I Chu^{1,2}

¹*Center for Quantum Science and Engineering, Department of Physics,
National Taiwan University, Taipei 10617, Taiwan and*

²*Department of Chemistry, University of Kansas, Lawrence, Kansas 66045, USA*

(Dated: July 17, 2022)

We propose an experimental feasible method for controlling the atomic currents of a two-component Bose-Einstein condensate in a double well by applying an external field to the atoms in one of the potential wells. We study the ground-state properties of the system and show that the directions of spin currents and net-particle tunneling can be manipulated by adiabatically varying the coupling strength between the atoms and the field. This system can be used for studying spin and tunneling phenomena across a wide range of interaction parameters. In addition, spin-squeezed states can be generated. It is useful for quantum information processing and quantum metrology.

PACS numbers: 03.75.Lm, 03.75.Mn, 05.60.Gg

Spin and tunneling phenomena are of fundamental interests in understanding quantum behaviors of particles. They are also important in the applications using solid-state devices such as sensors and data storage [1]. In addition, manipulation of the quantum state of a single spin is essential in implementing quantum information processing [2].

Recently, the tunneling dynamics of ultracold atoms has been observed in a double well [3] and optical lattices [4], where the experimental parameters can be widely tuned. Moreover, high-fidelity single-spin detection of an atom has been realized in an optical lattice [5, 6] and atom-chip [7], respectively. Such sophisticated techniques of manipulating ultracold atoms open up the possibilities for the study of intriguing quantum phenomena never possible before.

In this Letter, we propose a method to control the tunneling dynamics of a two-component Bose-Einstein condensate (BEC) in a double well [8] by applying an external field to the atoms in one of the potential wells. In fact, a number of methods for manipulating the atomic motions in an optical lattice have been proposed such as using external fields for vibrational transitions between adjacent sites [9], tilting the lattice potential [10] and periodic modulation of the lattice parameters [11]. Recently, a symmetry-breaking field [12] has been suggested to control the transport of atoms.

Here we show that the spin and tunneling dynamics of atoms can be manipulated by adiabatically changing the coupling strength of the field. This approach can be used for studying the spin and tunneling related phenomena in a controllable manner. For example, the directions of spin currents such as *parallel*- and *counter*-flows can be controlled by appropriately adjusting the interaction parameters. Apart from changing the internal states of atoms, the external field gives rise to *net-particle tunneling*. It is different to the situation of co-tunneling of the two component condensates in a double well [8, 13] in which the number difference of atoms between the wells

is equal during the tunneling process.

In addition, the tunnel behaviors are totally different in the limits of weak and strong atomic interactions. In the regime of weak atomic interactions, the atoms smoothly tunnel through the other well. On the contrary, the discrete steps of tunneling are shown in the limit of strong atomic interactions. The coherent control of single-atom tunneling can thus be achieved. This method can be utilized for atomic transport.

Furthermore, we investigate the production of spin squeezing [14, 15] in this system. The occurrence of spin-squeezing can indicate multi-particle entanglement [16]. We show that spin-squeezed states can be dynamically generated by slowly changing the coupling strength of the field. This can be used for preparing entangled states and quantum metrology [17].

We consider a condensate of ⁸⁷Rb atoms with two hyperfine levels $|e\rangle = |F = 2, m_F = 1\rangle$ and $|g\rangle = |F = 1, m_F = -1\rangle$ of the $5S_{1/2}$ ground state [18] confined in a symmetric double-well potential [8]. An external field is applied to the atoms in one of the potential wells. The schematic of the system is shown in Fig. 1(a). This system can be described by the total Hamiltonian $H_{\text{tot}} = H_{\text{ext}} + H_{\text{int}}$, where H_{ext} and H_{int} are the Hamiltonians describing the external and internal degree of atoms.

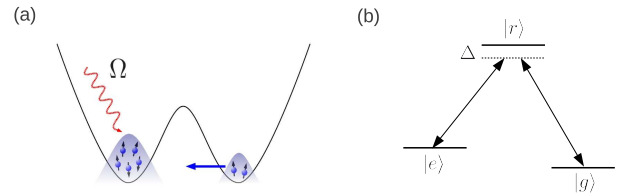


FIG. 1: (Color online) (a) Schematic of a two-component Bose-Einstein condensate in a double well. An external field is applied to the atoms in the left potential well. (b) Energy levels for the atoms. The two internal states $|e\rangle$ and $|g\rangle$ are coupled via the upper state $|r\rangle$.

We adopt the two-mode approximation to describe the atoms in deep potential wells [8]. Since the scattering lengths of the different hyperfine states of ^{87}Rb are very similar [20], we assume that the intra- and inter-component interactions are nearly the same. The Hamiltonian H_{ext} can be written as

$$H_{\text{ext}} = -\hbar J(e_L^\dagger e_R + e_R^\dagger e_L + g_L^\dagger g_R + g_R^\dagger g_L) + \hbar U[(n_{eL} + n_{gL})^2 + (n_{eR} + n_{gR})^2], \quad (1)$$

where $\alpha_L(\alpha_R)$ and $n_{\alpha L}(n_{\alpha R})$ are annihilation operator of an atom and number operator in the left(right) potential well, for $\alpha = e, g$. Note that the total number N of atoms is conserved in this system.

Without loss of generality, we consider an external field to be applied to the atoms in the left potential well. The two internal states can be coupled via the upper transition of the D_2 line of ^{87}Rb [21] as shown in Fig. 1(b). This upper state $|r\rangle$ can be adiabatically eliminated due to the large detuning. In the interaction picture, the Hamiltonian H_{int} is given by [19]

$$H_{\text{int}} = \hbar \Delta(n_{eL} + n_{eR}) + \hbar \Omega(e_L^\dagger g_L + \text{H.c.}), \quad (2)$$

where Δ is the detuning between the atomic transition ($|r\rangle$ and $|e\rangle$) and the laser field, and Ω is the effective coupling strength between the atoms and external field.

Now we study how the ground state properties of the BEC affected by the local external field. In Fig. 2, we plot the population differences ($\langle n_{\alpha L} \rangle - \langle n_{\alpha R} \rangle$) versus the coupling strengths Ω for the atoms in the two different internal states $|\alpha\rangle$ and $\alpha = e, g$. For the cases of even number N of atoms, there is an equal number of atoms in the two wells in the absence of the external field, i.e., $\Omega = 0$. The external field causes the energy bias between the two wells. Thus, the population difference becomes larger when the coupling strength increases.

Moreover, the system exhibits totally different behaviors in the regimes of weak and strong atomic interactions. For weak atomic interactions, the population differences smoothly vary as a function of the coupling strength as shown in Figs. 2(a) and (c). Also, a larger number of atoms are in the state $|g\rangle$ due to the larger detuning Δ .

In Figs. 2(b) and (d), we plot the population differences versus the coupling strengths Ω in the regime of strong atomic interactions. We can see that discrete steps of the population difference for atoms in the state $|g\rangle$ are shown when the coupling strength increases. However, the discrete feature is not obvious for the atoms in the state $|e\rangle$. In Fig. 2(b), the atoms, in the two different internal states, distribute in the opposite potential wells for small Ω . When Ω becomes larger, both component of atoms populate in the left potential well. This result shows that the population difference of atoms in the two internal states depends on the coupling strength and also the detuning between the atoms and field.

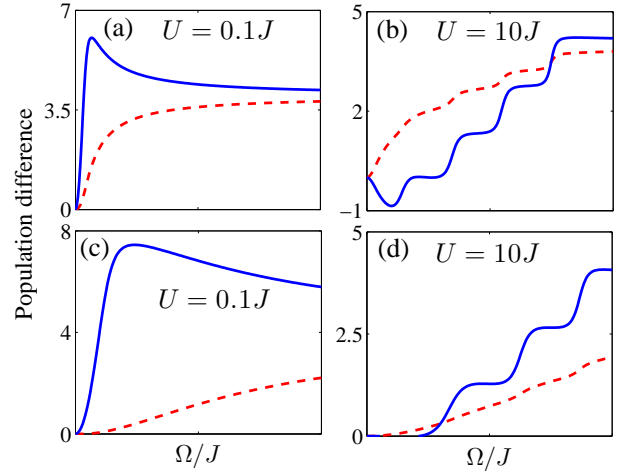


FIG. 2: (Color online) Population differences are plotted as a function of Ω/J for the ground state of the system and $N = 8$. The parameters are shown: (a) and (b) $\Delta = 20J$; (c) and (d) $\Delta = 200J$. The ground state $|g\rangle$ and excited state $|e\rangle$ of atoms are denoted by blue-solid and red-dotted lines, respectively.

To proceed, we investigate the relationship between the total population difference of atoms ($\langle n_{eL} + n_{gL} - n_{eR} - n_{gR} \rangle$) and the coupling strength Ω . In Fig. 3, we plot the total population differences as a function of the coupling strength Ω for different strengths U of atomic interactions. The external field leads to the population imbalance between two wells in both regimes of weak and strong atomic interactions. For weak atomic interactions, the population difference smoothly increases with Ω . When the atomic interactions become strong, the discrete steps of population differences are shown in Fig. 3. The sharper discrete steps are shown for larger U . In this case, a single atom is only allowed to tunnel through the other well for the specific coupling strengths.

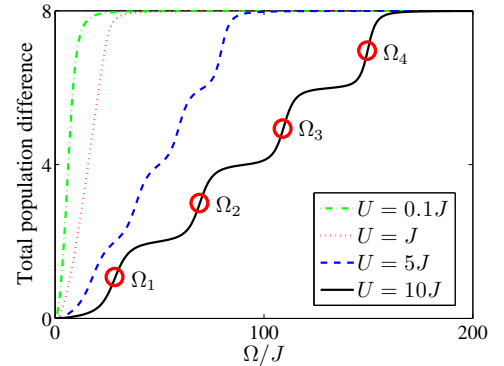


FIG. 3: (Color online) Plot of the total population difference versus Ω/J for the ground state with the different strengths U of atomic interactions. The parameters are used: $N = 8$ and $\Delta = 20J$. The values of Ω_n in Eq. (4) are marked with the red empty circles.

We now discuss the tunneling condition in the limit of strong atomic interactions. Since the tunnel couplings are negligible in this regime, the numbers of atoms in the two wells are conserved. We assume that there are $N/2 + n$ and $N/2 - n$ atoms in the left and right wells. For convenience, we define the angular momentum operators: $S_{jx} = (g_j e_j^\dagger + e_j g_j^\dagger)/2$, $S_{jy} = (g_j e_j^\dagger - e_j g_j^\dagger)/2i$ and $S_{jz} = (e_j^\dagger e_j - g_j^\dagger g_j)/2$, and $j = L, R$. To diagonalize the Hamiltonian H_{tot} , we apply the transformation as $S_{Lx} = \cos \theta S'_{Lx} - \sin \theta S'_{Lz}$ and $S_{Lz} = \cos \theta S'_{Lz} + \sin \theta S'_{Lx}$. By setting the term, $\Delta \sin \theta + 2\Omega \cos \theta$, to zero, the total Hamiltonian can be diagonalized as

$$H'_{\text{tot}} = \hbar \Delta S_{Rz} + \hbar \sqrt{\Delta^2 + 4\Omega^2} S'_{Lz} + \hbar U (N^2/2 + 2n^2) + \hbar \Delta N/2, \quad (3)$$

and its ground-state energy E_n^G is given by

$$E_n^G = -\hbar \Delta (N/2 - n)/2 - \hbar \sqrt{\Delta^2 + 4\Omega^2} (N/2 + n)/2 + 2\hbar U n^2 + \hbar U N^2/2 + \hbar \Delta N/2. \quad (4)$$

The tunneling of atoms occurs when the energies E_n^G and E_{n-1}^G are equal to each other. In this situation, a single atom tunnels through the other well. It is analogous to the resonant tunneling in quantum dots due to the Coulomb blockade [22]. By setting $E_n^G = E_{n-1}^G$ in Eq. (4), the tunneling condition for the coupling strength Ω_n can be obtained as

$$\Omega_n = \frac{1}{2} \{ [4U(2n-1) + \Delta]^2 - \Delta^2 \}^{\frac{1}{2}}. \quad (5)$$

In Fig. 3, the values of Ω_n are marked with the red empty circles. This shows that the tunneling condition in Eq. (5) agrees with the exact numerical solution.

Next, we study the adiabatic transition of the ground state of the system by slowly increasing the coupling strength Ω . We consider the coupling strength $\Omega(t)$ as a linear function of time t , i.e.,

$$\Omega(t) = vt, \quad (6)$$

where v is a positive number.

Initially, the system is prepared in its ground state for $\Omega = 0$. The coupling strength $\Omega(t)$ in Eq. (6) is adiabatically increased. According to the adiabatic theorem [23], the system can evolve as its instantaneous ground state if the changing rate of the parameter Ω is sufficiently slow. In Figs. 4(a) and (b), the population differences are plotted versus the time for the atoms in the different internal states. We can see that the two results in Figs. 2 and 4 reach a good agreement. This shows that the tunneling dynamics of atoms can be controlled by using an external field.

In the regime of weak atomic interactions, the two different component condensates smoothly tunnel through the other well in the same direction in Fig. 4(a). In the

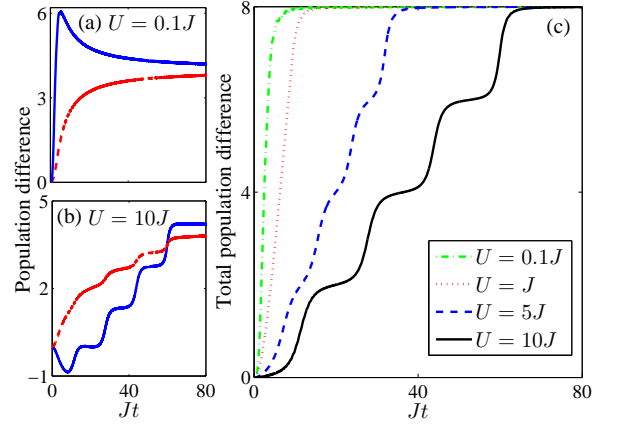


FIG. 4: (Color online) The population differences for the two different component condensates are plotted against the time Jt for $U = 0.1J$ and $10J$ in (a) and (b). The atoms in ground and excited states are denoted by blue-solid and red-dashed lines, respectively. (c) Plot of the total population difference versus the time Jt for different strengths of atomic interactions. The parameters are used: $N = 8$, $\Delta = 20J$ and $v = 2.5J$.

opposite interaction limit, the discrete steps are shown in Fig. 4(b). Note that the counter-flow is shown in a short time in figure (b). The flows of atomic spin currents become parallel afterward. This shows that the direction of spin flows can be controlled by appropriately adjusting the parameters Ω and Δ .

Then, we study the time evolution of total population difference of atoms. In Fig. 4(c), we examine the tunneling dynamics for a wide range of interaction parameters. In both regimes, the atoms tunnel to the left potential well when the coupling strength slowly increases with time. The total population differences smoothly increases as a function of time for weak atomic interactions. The discrete steps of the tunneling are shown when the strength of atomic interactions becomes strong. The single-atom tunneling can thus be achieved in the limit of strong atomic interactions.

Next, we investigate the efficiency of the population transfer by increasing the coupling strength of the external field. In Figs. 5(a) and (b), the population differences are plotted versus the time for the two different detunings $\Delta = 20J$ and $200J$. The full population transfer can be achieved if the parameters v are small enough in both cases. When the parameters v become larger, the rates of population transfer increase. However, the smaller population of atoms can be transferred in both cases. It is because they have gone beyond the adiabatic limit. By comparing the figures 5(a) and (b), we find that the larger numbers of atoms can be transported with the same rate v of change for the case using a larger detuning.

Having discussed the tunneling dynamics of atoms, we study the generation of spin-squeezed states by adiabatic

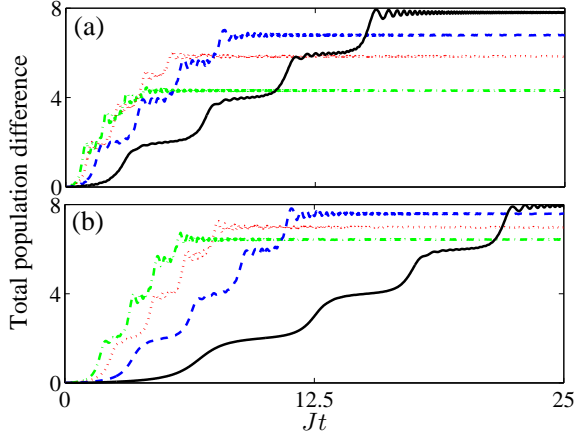


FIG. 5: (Color online) The total population differences are plotted versus the time Jt for the different detunings $\Delta = 20J$ and $200J$ in (a) and (b), respectively. The different rates of change are denoted: $v = 10J$ (black-solid line), $v = 20J$ (blue-dashed line), $v = 30J$ (red-dotted line) and $v = 40J$ (green-dashed-dotted line), respectively. The parameters are used: $N = 8$ and $U = 10J$.

ically changing the coupling strength of the field. To indicate the occurrence of spin squeezing, a parameter ξ^2 can be defined as [15]

$$\xi^2 = \frac{N(\Delta S_{n_1})^2}{\langle S_{n_2} \rangle^2 + \langle S_{n_3} \rangle^2}, \quad (7)$$

where n_i is the i -th component of an angular momentum system, and $i = 1, 2$ and 3 . If ξ is less than one, then the system is said to be spin-squeezed [15]. In addition, the parameter ξ can be used for indicating multi-particle entanglement [16].

Let us define the angular momentum operators as: $S_x = (e_L^\dagger e_R + g_L^\dagger g_R + e_R^\dagger e_L + g_R^\dagger g_L)/2$, $S_y = (e_L^\dagger e_R + g_L^\dagger g_R - e_R^\dagger e_L - g_R^\dagger g_L)/2i$, and $S_z = (e_L^\dagger e_R + g_L^\dagger g_L - e_R^\dagger e_R - g_R^\dagger g_R)/2$. The angular momentum operators obey the standard commutation rule. We study the parameter as

$$\xi^2 = \frac{N(\Delta S_z)^2}{\langle S_x \rangle^2}. \quad (8)$$

Physically speaking, the quantity $(\Delta S_z)^2$ is the variance of the total population difference of atoms between the wells, and $\langle S_x \rangle$ is the sum of the phase coherences between the two wells for the two component condensates.

In Fig. 6, we plot the spin-squeezing parameter ξ^2 versus the time for different number of atoms. Initially, the parameter ξ^2 is below one when $\Omega = 0$. This means that the initial ground state is a spin-squeezed state. As Ω in Eq. (5) slowly increases with time, spin squeezing can be dynamically produced. This result indicates that the system is spin-squeezed for a wide range of Ω . Besides, a higher degree of spin squeezing can be produced with a larger number of atoms N .

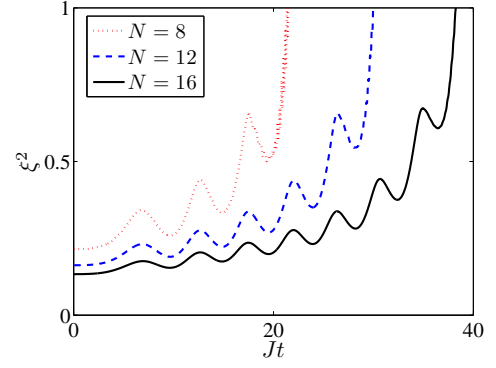


FIG. 6: (Color online) The spin-squeezing parameters ξ^2 are plotted versus the time Jt for different number N of atoms. The parameters are used: $\Delta = 200J$, $U = 10J$ and $v = 10J$.

In summary, we have studied how the ground state of a two-component condensate in a double well affected by a local external field. We have shown that the flows of spin currents and particle-tunneling dynamics can be controlled by slowly varying the coupling strength of the external field and appropriately adjusting the detuning. This can be used for studying spin and tunneling phenomena and also the potential applications of atomic devices in atomtronics [24]. In addition, spin-squeezed states can be dynamical generated. It is an important resource for precision measurement [14–16].

This work was partially supported by U.S. National Science Foundation. We would like to also acknowledge the partial support of National Science Council (Grant No. 100-2119-M-002-013-MY3) and National Taiwan University (Grant No. 10R1004021, 10R80914-1, 10R80700-2).

-
- [1] A. Fert, Rev. Mod. Phys. **80**, 1517 (2008).
 - [2] M. A. Nielsen and I. L. Chuang, *Quantum Computation and Quantum Information* (Cambridge University Press, Cambridge, 2000).
 - [3] M. Albiez, *et al.*, Phys. Rev. Lett. **95**, 010402 (2005).
 - [4] S. Fölling, *et al.*, Nature **448**, 1029 (2007).
 - [5] W. S. Bakr *et al.*, Nature **462**, 74 (2009).
 - [6] C. Weitenberg *et al.*, Nature, **471**, 319 (2011).
 - [7] J. Volz *et al.*, Nature **475**, 210 (2011).
 - [8] H. T. Ng, C. K. Law, and P. T. Leung, Phys. Rev. A **68**, 013604 (2003).
 - [9] L. Forster, *et al.*, Phys. Rev. Lett. **103**, 233001 (2009); Q. Beaufils *et al.*, *ibid.* **106**, 213002 (2011).
 - [10] D. R. Dounas-Frazer, A. M. Hermundstad and L. D. Carr, Phys. Rev. Lett. **99** 200402 (2007); P. Cheinet *et al.*, *ibid.* **101**, 090404 (2008).
 - [11] C.E. Creffield, Phys. Rev. Lett., **99**, 110501 (2007); O. Romero-Isart and J. J. García-Ripoll, Phys. Rev. A **76**, 052304 (2007); Y. Qian, Ming Gong and C. Zhang, *ibid.* **84**, 013608 (2011).

- [12] L. Morales-Molina and J. Gong, Phys. Rev. A **78**, 041403(R) (2008).
- [13] A.B. Kuklov and B.V. Svistunov, Phys. Rev. Lett. **90**, 100401 (2003).
- [14] M. Kitagawa and M. Ueda, Phys. Rev. A **47**, 5138 (1993).
- [15] D. J. Wineland, J. J. Bollinger, W. M. Itano and D. J. Heinzen, Phys. Rev. A **50**, 67 (1994).
- [16] A. Sorensen, L.-M. Duan, I. Cirac, P. Zoller, Nature **409**, 63 (2001).
- [17] J. Estève *et al.*, Nature **455**, 1216 (2008); M. F. Riedel *et al.*, *ibid.* **464**, 1170 (2010).
- [18] D. M. Harber *et al.*, Phys. Rev. A **66**, 053616 (2002).
- [19] S. M. Barnett and P. M. Radmore, *Methods in Theoretical Quantum Optics* (Oxford University Press, Oxford, 2002).
- [20] M. R. Matthews *et al.*, Phys. Rev. Lett. **81**, 243 (1998).
- [21] D. A. Steck, Rubidium 87 D line data, <http://steck.us/alkalidata/> (2010)
- [22] C. W. J. Beenakker, Phys. Rev. B **44**, 1646 (1991).
- [23] A. Messiah, *Quantum Mechanics* (Dover, New York, 1999).
- [24] R. A. Pepino, J. Cooper, D.Z. Anderson and M. J. Holland, Phys. Rev. Lett. **103**, 140405 (2009).